Iranian Journal of Chemical Engineering
Vol. 7, No. 3 (Summer), 2010, IAChE

Investigation of Temperature and Flow Fields in an Alternative Design of Industrial Cracking Furnaces Using CFD

J. Aminian[1], Sh. Shahhosseini[1], M. Bayat[2]*

1- School of Chemical Engineering, Iran University of Science and Technology (IUST), Narmak, Tehran, Iran
2- Research Institute of Petroleum Industry (RIPI), Petroleum Refining Division, West Blvd., Azadi Sports Complex, Tehran, Iran

Abstract

Enhanced design strategies in the industrial cracking furnaces are of practical interest for petrochemical industries. For such engineering purposes the exact simulation of temperature and flow fields in the furnace is mandatory. In this paper, a study was conducted to simulate 3D flue gas flow pattern and temperature field in the radiation section of an industrial cracking furnace in order to improve the design of the steam cracking furnaces, employing the computational fluid dynamics (CFD) technique. The steady-state Reynolds averaged Navier–Stokes (RANS) equations were solved, in a finite volume scheme for a turbulent premixed flow applying the renormalization group (RNG) version of the $k-\varepsilon$ model, together with global combustion kinetics for methane-hydrogen-air. Calculation of the Damkhöler number and optical-thickness was conducted to identify the appropriate methods for the numerical modeling of radiation and turbulence-chemistry interaction phenomena. The predicted results match the literature data quite well. The validated numerical procedure was then employed to investigate alternative design attributed to different burner locations. The alternative design resulted in a more uniform temperature profile on the reactor tubes as well as lower peak flame temperature.

Keywords: *CFD, Cracking Furnace, Combustion, Radiation, Turbulence-Chemistry Interaction*

1- Introduction

Thermal cracking of hydrocarbons is an endothermic process that takes place in tubular reactor coils suspended in large gas-fired furnaces. The heat is transferred to the reactor tubes, mainly due to the radiation from the furnace refractory walls and the recirculated flue gas. In general, the combustion fuel gas is to be equally distributed over all reactor tubes in the furnace [1]. The process gas that flows through the coils is heated up to high temperatures by means of gas-fired long flame burners distributed on the floor or gas-fired radiation burners located on the side walls of the furnace. Increasing demand in quality improvement, energy saving and the emission control of pollutants urge industries

∗ Corresponding author: shahrokh@iust.ac.ir

to optimize their furnaces [2]. A number of studies have been conducted to investigate thermal efficiency in the industrial cracking furnaces [1-5].

Heynderickx et al. have developed a three-dimensional finite-volume package for the coupled simulation of furnace and reactor sides of a naphtha cracking furnace [1]. They employed a five-step reaction mechanism for the combustion of methane in flame and a detailed radical reaction scheme, containing over 1000 reactions between 128 species, for the cracking of hydrocarbons. A rate expression coke-formation model, developed by Reyniers et al. [6], has also been coupled with the one-dimensional reactor model. The calculation of the heat fluxes to the reactor tubes was performed based on the zone method of Hottel and Sarofim [7]. The turbulent properties have been calculated using the $k-\varepsilon$ turbulence model. They reported an extremely uneven distribution of the flue gas over the two furnace halves due to the asymmetric position of the flue-gas outlet. Furthermore, the calculated flow profiles revealed a flue-gas "shortcut" flow between the outer reactor tubes of the reactor tube row and the short furnace walls [1].

Van Geem et al. have employed a two-dimensional reactor model coupled with a coke-formation model to investigate the effect of radial temperature profile on the yield of ethylene cracking furnaces [2]. They showed that the radial temperature gradient in reactor tubes causes the conversion of light olefins to heavier ones, therefore decreasing the ethylene production yield. They have also reported, only when the coke model is coupled to a two-dimensional reactor model (axial and radial), good agreement with the experimental data can be achieved [2].

Circumferential temperature profile (azimuthal gradient) also has some effects on the cocking rate in the reactor tubes [8]. Heynderickx et al. have employed one-dimensional (axial) reactor model together with a peripheral discretization of the reactor tube walls to investigate the influence of circumferential temperature profile on the cocking rate in cracking furnaces [8]. They showed that, even with a single row of coils the difference between the maximum and minimum peripheral temperature can be of the order of 50°C. They reported that this non-uniformity can affect the furnace run-length production cycle which is often dictated by the maximum allowable tube skin temperature and coils pressure drop.

Habibi et al. have simulated turbulent combustion in an industrial steam cracking furnace using a three-dimensional RANS approach together with a $RNG\,k-\varepsilon$ turbulence model and EDC as the turbulence-chemistry-interaction (TCI) method [3]. The WSGG model has been employed to calculate radiative properties in the P-1 and DO radiation models. The amount of thermal, prompt and N_2O-intermediate NO_x mechanisms has also been investigated in the post-processing stage. Calculation of the Damköhler number reveals that the combustion regime in the furnace is a "corrugated flamelet regime", which emphasis the validity of fast-chemistry assumption in furnaces. They distinguished three different regions including, the preheat region (very small), combustion region (anchored at the jet inlet), and the post-combustion region, where heat is transferred

from the hot flue gases toward the walls and tubes. In addition, it was approved that thermal NO formation is by far the most important mechanism in the NO_x chemistry [3].

In another study, Habibi et al. evaluated the effect of three different radiation models (Rosseland, P-1 and DO) on the predicted wall, tube skin and flue gas temperature profiles and heat fluxes towards the reactor tubes, as well as on the predicted species concentration profiles and flame structure under normal firing conditions of the same industrial steam cracking furnace [4]. They concluded that the Rosseland model is not appropriate for radiation modelling in furnaces, since it could not properly predict the reaction zone location. It was shown that the results with the P-1 and DO radiation models are very similar. However, according to the calculated optical-thickness values, the DO model was recommended since it is applicable to all ranges of optical-thicknesses even with a higher computational cost [4].

Stefanids et al. have investigated the possibility of improving the efficiency of steam cracking furnaces due to the application of high-emissivity coatings on the furnace walls [9]. They reported that applying a high-emissivity coating on the furnace wall has decreased the net absorption of radiation by the flue gases and resulted in increased radiation from the furnace wall to the reactor tubes. It has been shown that application of a high-emissivity coating on the furnace walls improves the thermal efficiency of the furnace by 1%, the naphtha conversion by 1% and the ethylene yield by 0.5% [9].

So far, no systematic study has been carried out to investigate alternative designs aimed at finding different burner locations in order to revamp the long-flame burner cracking furnaces. In the present study, three-dimensional CFD simulation of flow, temperature and concentration fields for the radiation section of an industrial scale thermal cracking furnace is presented consisting of two major parts. The first part is aimed at determination of the appropriate turbulence-chemistry interaction (TCI) and radiation models for the numerical simulation of industrial combustion. In the second part, an alternative design was investigated to improve the thermal efficiency of the cracking furnace.

2- Regimes of premixed turbulent combustion

An important dimensionless parameter in combustion is the Damköhler number (Da). This parameter appears in the description of many combustion problems and is quite important in understanding turbulent premixed flames [10]. The fundamental meaning of the Damköhler number is that it represents the ratio of the turbulent time scale to the chemical time scale as follows:

$$Da = \frac{\tau_{Turb.}}{\tau_{Chem.}} \tag{1}$$

The evaluation of the Damköhler number depends on the situation under study. For our study of premixed combustion, useful characteristic time scales are the lifetime of large eddies in the flow (Eq. (2)) and the chemical time based on a laminar flame (Eq. (3)).

$$\tau_{Turb.} = \frac{\ell_0}{v'_{rms}} \tag{2}$$

$$\tau_{Chem.} = \frac{\delta_L}{S_L} \quad (3)$$

Where, ℓ_0 is the integral scale characterizing the largest eddy sizes, v'_{rms} is the fluctuations of the velocity field and δ_L and S_L are the laminar flame thickness and burning velocity respectively.
The size of large eddies may be written as [11]:

$$\ell_0 = \frac{v'^3_{rms}}{\varepsilon} \quad (4)$$

Where, v'^3_{rms} and ε are the velocity fluctuation and dissipation rate of kinetic energy respectively. When $Da >> 1$, the time needed for fluid mixing is greater than the chemical reaction rates and a fast-chemistry regime is defined. Conversely, when the reaction rate is in the same order of the mixing rate, then $Da \approx 1$ and both turbulent mixing and chemical reactions must be considered via an appropriate TCI model. A review of different fast-chemistry and finite-rate chemistry approaches may be found elsewhere [5].

3- Radiation modeling approaches

The main challenges of radiation modeling in combustion problems are handling the radiative properties of the medium and solving the radiative transfer equation (RTE). Two extreme approaches for the former issue are the oversimplified gray gas model and the complete model which takes into account particular absorption bands. The first approach jeopardizes the solution accuracy, while the next imposes enhanced computational cost. Weighted-sum-of-gray-gases (WSGG) model is a reasonable compromise between the above mentioned extremes. In this method, the non-gray gas is replaced by a number of gray gases for which the radiation heat transfer rates are calculated independently. The total heat flux is then found by summation of the heat fluxes after multiplication with certain weight factors [12]. According to Eq. (5), the WSGG model accounts for spatial variation in total emissivity (or absorptivity) as a function of the gas composition and temperature.

$$\alpha(T, S) \approx \sum_{i=1}^{N} a_i(T)\left[1 - e^{-\kappa_i S}\right] \quad (5)$$

where, a_i, κ_i and S are weighting factors, absorption coefficient of the *i*th gray gas and path length respectively. Weighting factors and absorption coefficients depend on the gas composition. The first one also varied with temperature [13].
The radiative transfer equation (RTE) for an absorbing, emitting and non-scattering medium at position $\vec{r}$ in the direction $\vec{s}$ is given as follows [12]:

$$\frac{dI(\vec{r},\vec{s})}{ds} = -\alpha I(\vec{r},\vec{s}) + \alpha n^2 \frac{\sigma T^4}{\pi} \quad (6)$$

where α, I, n, σ and T represent total absorptivity calculated using Eq. (5), radiation intensity, refractive index, Stefan-Boltzman constant $\left(= 5.672 \times 10^{-8} W/m^2 K^4\right)$ and local temperature respectively. The RTE comprises seven independent variables: three spatial coordinates $(\vec{r})$, two angular

coordinates $(\vec{s})$ which define the direction of propagation, one spectral variable (α) and time. The dependence on time is negligible for most practical applications, including turbulent reactive flows, because a radiation beam travels at the speed of light, which exceeds the typical velocities in such flows by several orders of magnitude [14]. Many methods are available to solve the RTE such as the Roseland, P-1 and discrete ordinates (DO) methods [12]. A comparative description of these methods may be found in the study done by Habibi et al. [4]. Here, we do not describe these methods, but in the following paragraph a practical concept will be discussed as a criterion for choosing the appropriate RTE solving method.

Optical-thickness (Eq. (7)) is a good indicator of which RTE solving method to use in a specific combustion problem [10].

$$OP = \kappa \times L \tag{7}$$

Here, κ is the local mean absorption coefficient and L is an appropriate length scale for the computational domain. There is a general agreement that in the turbulent premixed combustion, chemical reactions take place in the turbulent scales larger than the flame thickness [15]. Therefore, it can be concluded that the size of large eddies is a good candidate for the length scale in Eq. (7). Substituting $v'_{rms} = \sqrt{2k/\rho}$ into Eq. (4), the size of large eddies may be calculated as follows:

$$\ell_0 = \frac{(2k/\rho)^{3/2}}{\varepsilon} \approx \frac{k^{3/2}}{\varepsilon} = L \tag{8}$$

For a weak medium $(OP < 1)$ little absorption takes place, so that every position in the medium receives the full irradiation resulting in a linear absorption rate with distance. In the case of a strong medium $(OP > 1)$, the radiation intensity has been appreciably weakened before exiting the medium, resulting in locally lesser absorption and causing square root dependence on distance [12]. If $OP > 1$, the best RTE solving methods are the P-1 and Rosseland methods. In particular the P-1 model should be used for optical thicknesses larger than 1. For an optical thickness larger than 3, the Rosseland model is cheaper and more efficient. The Discrete Ordinates (DO) model works across the range of optical thicknesses. However, it is substantially more computationally expensive than the Rosseland and P-1 models [12].

4- Numerical modeling of steam cracking furnace

The 3D computational domain of an industrial steam cracking furnace is shown in Fig. 1. The segment contains two flame burners that are positioned on the left and the right side of six reactor tubes. Fuel (CH_4/H_2) and air are premixed before entering the radiation section. The mixture composition is 94.3% CH_4 and 5.7% H_2 by weight. Details of the industrial geometry may be found elsewhere [4, 5].

4.1- Turbulence modeling

The steady-state Reynolds averaged Navier–Stokes (RANS) equations were solved, in a finite volume scheme, for a turbulent flow applying the $RNG\,k-\varepsilon$ turbulence model

[16]. The $RNG\,k-\varepsilon$ model (Eqs. (9) and (10)) has been derived using a rigorous statistical technique called renormalization group theory.

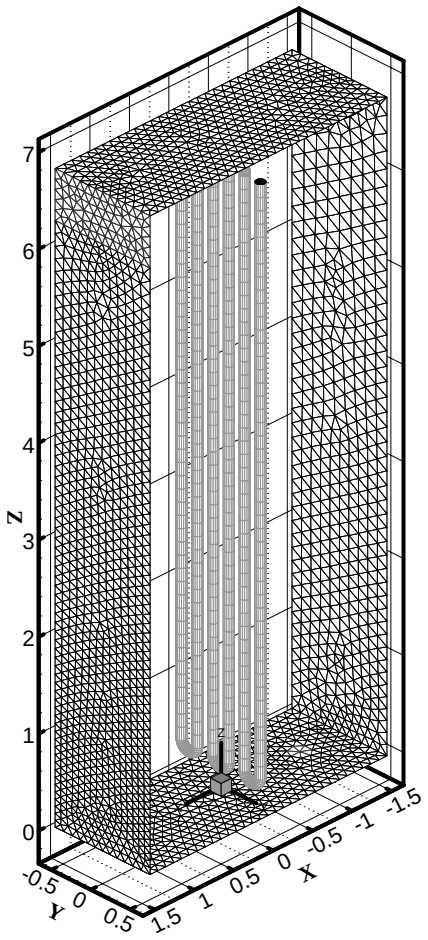

Figure 1. Computational domain and dimensions (m)

$$\rho\frac{\partial k}{\partial t}+\rho u_j k_{,j}=\left(\mu+\frac{\mu_t}{\sigma_k}k_{,j}\right)_{,j}+G+B-\rho\varepsilon \tag{9}$$

$$\rho\frac{\partial \varepsilon}{\partial t}+\rho u_j \varepsilon_{,j}=\left(\mu+\frac{\mu_t}{\sigma_\varepsilon}\varepsilon_{,j}\right)_{,j}+C_1\frac{\varepsilon}{k}G$$
$$+C_1(1-C_3)\frac{\varepsilon}{k}B-C_2\rho\frac{\varepsilon^2}{k}-\frac{C_\mu\eta^3\left(1-\eta/\eta_\circ\right)}{1+\beta\eta^3}\frac{\varepsilon^2}{k} \tag{10}$$

It is similar in form to the standard $k-\varepsilon$ model, but has an additional term in its ε equation (last term in Eq. (10)) that significantly improves the accuracy for rapidly strained flows [17]. The model constants C_1, C_2, C_μ, β and η_0 are equal to 1.42, 1.68, 0.0845, 0.012 and 4.38, respectively, which have been derived analytically by the RNG theory. σ_k and σ_ε are also the turbulent Prandtl numbers for k and ε equations equal to 0.7179.

Second-order upwind scheme is applied for the space derivatives of the advection terms in all transport equations. The SIMPLE algorithm is employed to handle velocity-pressure coupling in flow field equations [18]. An unstructured triangular meshing scheme is used to discretize the domain into 162471 cells. Standard wall functions are used as turbulent wall boundary conditions. At the burner inlets, the mass flow, temperature and mixture composition are imposed and at the furnace exit, the outlet pressure is imposed. A problem of realistic large-scale furnace simulations is the lack of available experimental data. Therefore, we discuss the simulation here based on the results reported by Stefanidis et al. [5].

4.2- Radiation modeling

To determine the appropriate radiation model for our simulation the local value of optical thickness throughout the furnace was evaluated. Figure 2 illustrates the contour of optical thickness in the middle of the furnace (plane Y=0 m). The optical thickness in the flame zone is rather low, but in the upper part the values become in the order of unity.

This explains why the P-1 and DO models are applicable for radiation modeling in the furnace. To reduce the CPU time associated with numerical simulation, the P-1 radiation model was adopted. It also incorporates the WSGG model in which spatial variation in the total emissivity is computed as a function of gas composition and temperature.

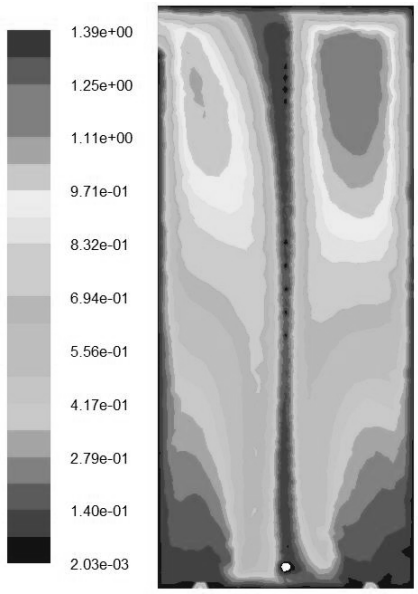

Figure 2. Contour of the optical thickness for DO radiation model in plane Y = 0 m

4.3- Combustion modeling

The following reaction scheme with corresponding intrinsic reaction rates are considered for the combustion of the CH_4/H_2/air mixture [4]:

$$CH_4 + 1.5O_2 \rightarrow CO + 2H_2O \quad ;$$
$$r_{CH_4} = 1.5\times10^{13} e^{-125604/RT} C_{CH_4}^{-0.3} C_{O_2}^{1.3}$$
$$CO + 0.5O_2 \rightarrow CO_2 \quad ;$$
$$r_{CO} = 3.98\times10^{20} e^{-167472/RT} C_{CO} C_{H_2O}^{0.5} C_{O_2}^{0.25}$$
$$H_2 + 0.5O_2 \rightarrow H_2O \quad ;$$
$$r_{H_2} = 1.0\times10^{13} C_{O_2}^{0.5} C_{H_2}$$

The kinetic parameters for the two-step methane combustion mechanism were derived by Westbrook and Dryer [19]. The reaction rate for hydrogen combustion was also reported with good results in different experiments [20, 21].

Capturing the effect of turbulence on the average reaction rates is an important issue of turbulent combustion modeling. Several approaches have been proposed to model the problem of turbulence–chemistry interactions (TCI) in combustion applications [15]. Those approaches were classified as fast-chemistry and finite-rate chemistry approaches. No matter which category, all of the TCI models (except the flamelet model) attempt to calculate, in some manner, the net rate of production of species i by chemical reaction (R_i) in the following mass transport equation [22]:

$$\frac{\partial}{\partial t}(\rho Y_i) + \nabla.(\rho u Y_i) = -\nabla.J_i + R_i \qquad (11)$$

where, ρ is the mixture density, Y_i is the mass fraction of species i, u is the velocity vector and J_i is the diffusion flux of species i due to concentration gradients.

As mentioned in section 2, the first step to evaluate the combustion regime is the calculation of the Damköhler number according to Eq. (1). For the calculation of the chemical time-scale the laminar flame thickness and laminar burning velocity are needed. In the case of methane-hydrogen-air flames some data is available in the literature. Coppens et al. proposed a correlation (Eq. (12)) for laminar burning velocity which takes into account the hydrogen content in the fuel [23]. In Eq.

(12), the shift of the maximum burning velocity due to the hydrogen addition to methane is considered in the exponent term. R_{H_2} and ϕ are hydrogen mass fraction and equivalence ratio respectively.

$$S_L = \left[1+1.9153R_{H_2}^{1.533}\right] \times 39.0542\phi^{-0.4333}e^{-6.0157\left(\phi-1.1-0.0133R_{H_2}\right)^2} \quad (12)$$

The laminar flame thickness is calculated applying Eq. (13) [10]:

$$\delta_L \cong \frac{2\alpha_T}{S_L} \quad (13)$$

where, α_T is the laminar thermal diffusivity. Consequently, the Damköhler number is calculated employing Eqs. (1), (2), (3), (4), (12) and (13). Figure 3, represents the contour plot of the Damköhler number through the furnace in plane Y=0 m.

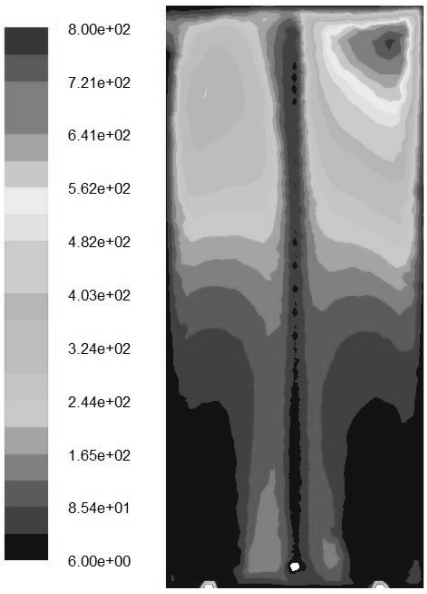

Figure 3. Contour of the Damköhler number employing eddy dissipation model in plane Y = 0 m

It can be observed that the Damköhler number in the flame zone is about 6 and increases to about 800 in the upper part of the furnace. In other words, based on the definition of Eq. (1), the turbulent time scale is definitely larger than the chemical time scale throughout the furnace. It can be concluded that the fast-chemistry assumption is an appropriate option to model turbulence-chemistry interactions (TCI) in steam cracking furnaces. Therefore, the eddy dissipation model (EDM) developed by Magnussen and Hjertager is employed in the present study. The model assumes that fuels are fast burning and the overall rate of reaction is controlled by turbulent mixing.

4.4- Model validation

Due to the lack of industrial experimental data, the numerical simulation results of this work have been validated against the numerical simulation results reported by Habibi et al [4]. They have implemented a finite-rate TCI model (FR/ED), which calculates both chemical and mixing rates and uses the smallest one, to consider turbulence-chemistry interaction in the furnace. Figure 4 provides a comparison for gas temperature profile in a vertical cross section between the predicted and reported data. The vertical temperature profiles are those calculated along the centerline of the right hand side burner (X=-1 m, Y=0 m). As can be seen, prediction of the CFD model together with the P-1 radiation model and EDM combustion model match the literature data [4] quite well. The maximum predicted gas temperature is obtained 1933 K at a height of Z= 1.17 m, which are in a good agreement with the literature data. Since the

EDM model (fast chemistry assumption) can follow the behavior of the FR/ED model (finite-rate chemistry assumption) quite well, it can be proved that this combustion regime is mixing dominant and fast chemistry assumption is justified.

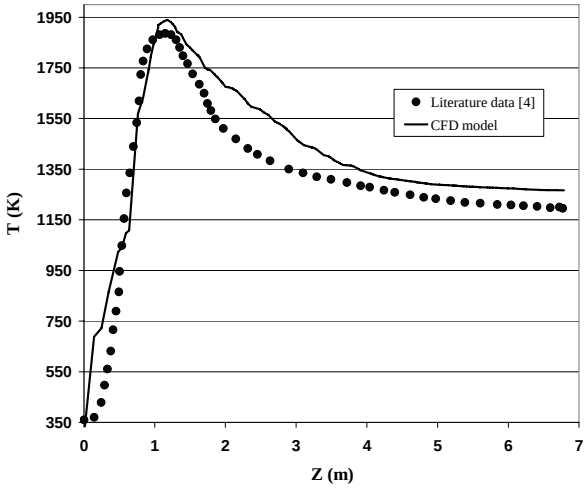

Figure 4. Evolution of the gas temperature in plane *Y*= 0 m above the right-hand side burner

To perform an in-depth evaluation of our numerical results, the simulated profiles of species concentration were plotted in Fig. 5 against the reported results by Habibi et al. [4].

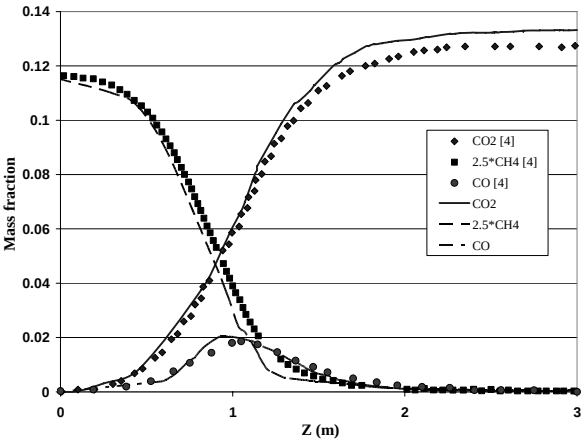

Figure 5. Species concentration profile in plane Y = 0 m above the right-hand side burner

A little over-prediction of CO_2 in Fig. 5 arises from temperature over-prediction in Fig. 4, which confirms the consistency of the numerical results.

4.5- Alternative design

In previous sections, a systematic study was adopted to determine the appropriate radiation and turbulence - chemistry interaction models for CFD modeling of steam cracking furnaces. Temperature profiles in the furnace, and therefore the type of burner that is used, influences radiation profiles to the reactor tubes. The standard geometry of cracking furnaces is the long-flame burner type, presented in previous sections, which is widely used in the olefin production industry. Long-flame burners lead to produce hot spots on the reactor tube walls. These hot spots are detrimental to the lifetime of the tubes and result in higher coking rates. The flue gas temperature distribution around the reactor tubes is important because it determines the heat flux towards the tubes and the tube skin temperature profile. Fig. 6 shows two large recirculation zones that are predicted in the upper right part and the lower core, which are similarly reported by Habibi et al. [4] and Stefanidis et al. [5]. These recirculation zones are obstructions for the flue gas flow and are due to the symmetric burners, position and flow rate, and asymmetric outlet of the flue gas in the furnace.

Due to the high residence time of the flue gas in the recirculation zone, the temperature in this region becomes uniform and lower. In the alternative design (Fig. 7) we simply add another burner to the top right hand side of the furnace. It should be noted that fuel

consumption was not increased and the previous flow rate was divided equally between the bottom and top right hand side burners (0.2113 kg/s). Fig. 8 illustrates the velocity profile in the alternative design. It can be observed that employing the third burner has two major effects on the flow of flue gas inside the furnace. First, the recirculation zone in the lower core of the first design (Fig. 6) has disappeared due to the unequal fuel flow rates of the fuel/air mixture in the lower burners. In Fig. 8, the right hand burner has a flow rate of 0.2113 kg/s, whilst the left hand burner flow rate has been kept unchanged (0.4226 kg/s). Second, the recirculation dead zone in the upper right part of the first design (Fig. 6) was destroyed due to the third burner. The third burner also improved the radiative fluxes and the tube skin temperature profile.

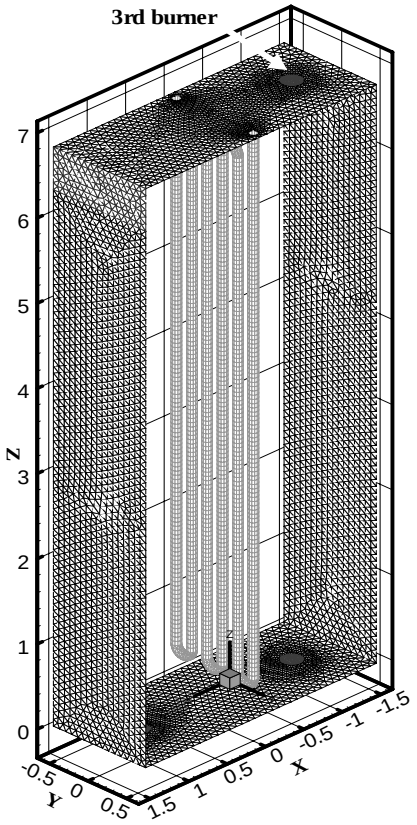

Figure 7. Alternative design

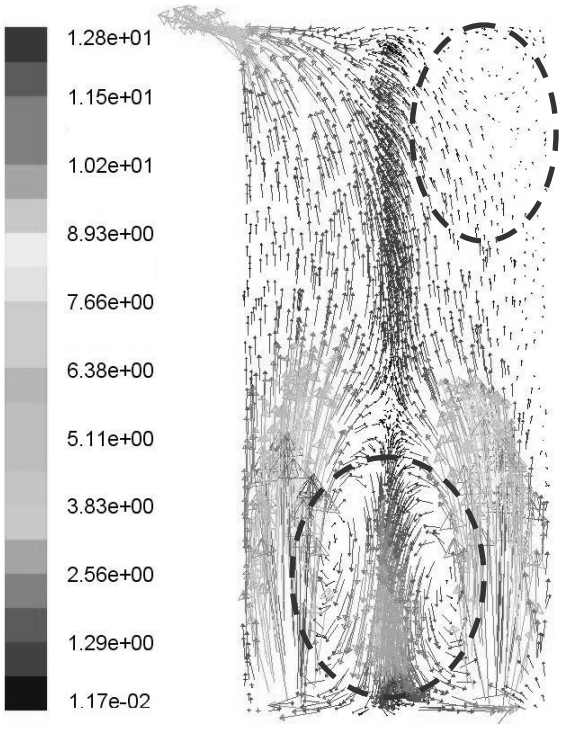

Figure 6. Vector plot of velocity profile in the first design

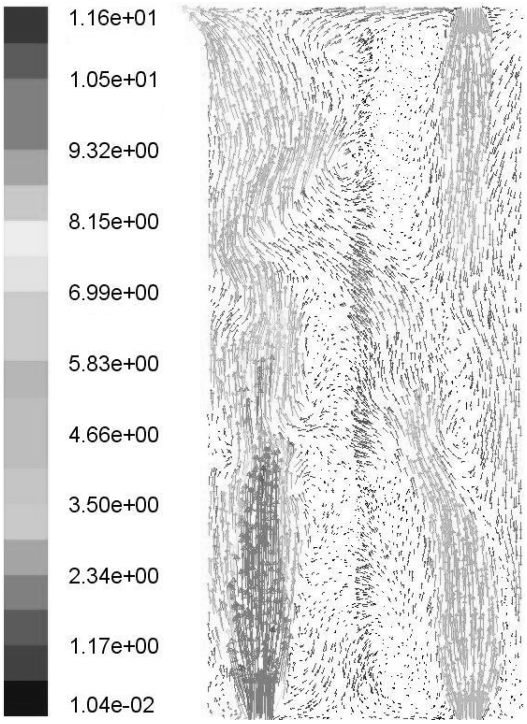

Figure 8. Vector plot of velocity profile in the second design

The temperature distribution in the middle of a plane adjacent to the reactor tubes for the first and alternative designs is shown in Fig. 9. It can be observed that improving recirculation of the flue gas and employing another burner on the top of the furnace has a significant effect on the tube skin temperature distribution. It is shown that the temperature on the reactor tubes changes between 1115 and 1257 K for the first design, which is in reasonable agreement with the experimental data reported by Stefanidis et al. [5]. However, the temperature field in the alternative design varies from 1149 to 1191 K. The first advantage of the alternative design is that the temperature field is more uniform throughout the furnace. This subsequently leads to a more even heating on the reactor tubes and therefore a uniform conversion of the process gas along the reactor tubes. The other benefit is the lowering of the maximum temperature on the reactor tubes which reduces the presence of hot spots on the tube walls.

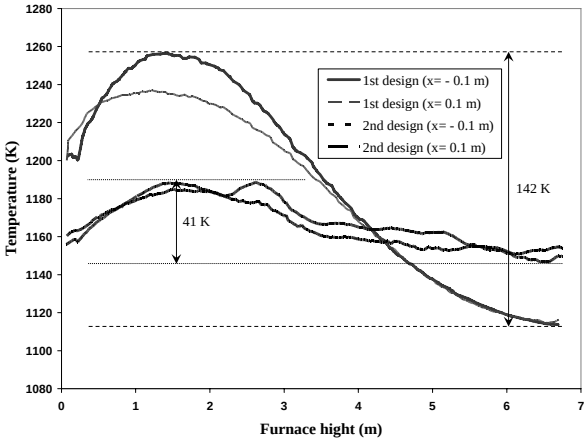

Figure 9. Temperature distribution on a plane adjacent to the reactor tubes

The results of the alternative design presented here, have illustrated improved temperature uniformity on the reactor tubes compared to the classical furnace design.

5- Conclusions

A 3D computational fluid dynamics model containing equations for mass, heat and momentum transfer together with an $RNG\,k-\varepsilon$ turbulence model was solved to calculate the 3D flue gas flow pattern and the corresponding 3D temperature field in an industrial steam cracking furnace. A systematic study was adopted to determine the appropriate radiation and turbulence-chemistry interaction models. It was found that the P-1 and DO solution methods are suitable for solving the RTE in industrial cracking furnaces, which are optically thin media. Calculation of the Damköhler number also demonstrated that a fast-chemistry model, like the EDM, is a reasonable assumption for modeling turbulence-chemistry interactions in cracking furnaces. Results showed a reasonable agreement between the experimental data and model predictions. An alternative design was also simulated to investigate the improvement of flue gas recirculation and temperature distribution throughout the furnace. The alternative design resulted in a more uniform temperature profile on the reactor tubes as well as a lower peak flame temperature. The former will subsequently lead to a more uniform conversion of the process gas along the reactor tubes and the latter may reduce the presence of hot spots on the tube walls. In future researches, the effect of new temperature and flow fields on pollutant formation can be studied, so that a more in-

depth evaluation of the alternative design can be performed.

6- Nomenclature

Roman symbols

α	total absorptivity
α_T	Laminar thermal diffusivity
κ	local mean absorption coefficient
κ_i	absorption coefficient of the i^{th} gray gas
μ_t	turbulent viscosity
μ	laminar viscosity
ε	dissipation rate of kinetic energy
ρ	density
σ	Stefan-Boltzman constant
ϕ	equivalence ratio
$\tau_{Turb.}$	turbulent time scale
$\tau_{Chem.}$	chemical time scale
ℓ_0	integral length scale (=largest eddy size)
v'_{rms}	velocity fluctuations
δ_L	laminar flame thickness

Letters

a_i	weighting factor of the i^{th} gray gas
B	generation of turbulent kinetic energy due to buoyancy
DO	discrete ordinates
Da	Damköhler number
EDM	eddy dissipation model
G	production of turbulent kinetic energy due to velocity gradients
I	radiation intensity
Ji	diffusion flux of species i
k	production rate of kinetic energy
L	domain length scale
n	refractive index
OP	optical-thickness
Ri	net rate of production of species i by chemical reaction
r	reaction rate
$\vec{r}$	spatial coordinates
RANS	Reynolds averaged Navier–Stokes
RHT	radiative heat transfer
RTE	radiative transfer equation
RNG	renormalization group
R_{H_2}	hydrogen mass fraction
S	path length
$\vec{s}$	angular coordinates
S_L	laminar burning velocity
T	local temperature
TCI	turbulence-chemistry interaction
WSGG	weighted sum of gray gases
Y_i	mass fraction of species i

References

[1] Heynderickx, G. J., Oprins, M., Marin, G. B., Dick, E., "Three-Dimensional flow patterns in cracking furnaces with long-flame burners", *AIChE J.,* **47** (2) 388, (2001).

[2] Van Geem, K. M., Heynderickx, G. J., Marin, G. B. "Effect of radial temperature profiles on yields in steam cracking", *AIChE J.,* **50** (1) 173, (2004).

[3] Habibi, A., Merci, B., Heynderickx, G. J., "Multiscale modeling of turbulent combustion and NOx emission in steam crackers", *AIChE J.,* **53** (9), 2384, (2007).

[4] Habibi, A., Merci, B., Heynderickx, G. J., "Impact of radiation models in CFD simulations of steam cracking furnaces", *Comp. Chem. Eng.,* **31**, 1389, (2007).

[5] Stefanidis, G. D., Merci, B., Heynderickx, G. J., Marin, G. B., "CFD simulations of steam cracking furnaces using detailed combustion mechanisms", *Comp. Chem. Eng.*, **30**, 635, (2006).

[6] Reyniers, G. C., Froment, G. F., Kopinke, F. D., Zimmerman, G. "Coke formation in the thermal cracking of hydrocarbons, 4. Modeling of coke formation in naphtha cracking", Ind. Eng. Chem. Res., 33, 2584, (1994).

[7] Hottel, H. C., Sarofim, A. F., Radiative heat transfer, McGraw-Hill, New York, (1967).

[8] Heynderickx, G.J., Cornelis, G.G., Froment, G.F., "Circumferential tube skin temperature profiles in thermal cracking coils", *AIChE J.*, **38** (12) 1905, (1992).

[9] Stefanidis, G.D., Van Geem, K.M., Heynderickx, G.J., Marin, G.B., "Evaluation of high-emissivity coatings in steam cracking furnaces using a non-grey gas radiation model", *Chem. Eng. J.,* **137**, 411, (2008).

[10] Turns, S. R., An introduction to combustion, 2nd ed., McGraw-Hill, p. 267, (2000).

[11] Veynante, D., Vervisch, L., "Turbulent combustion modeling", *Prog. Energy Comb. Sci.*, **28**, 193, (2002).

[12] Modest, M. F., Radiative heat transfer, 2nd ed., Academic Press, p. 424, (2003).

[13] Smith, T. F., Shen, Z. F., and Friedman, J. N., "Evaluation of coefficients for the weighted sum of Gray Gases Model", *J. Heat Transfer,* **104**, 602, (1982).

[14] Coelho, P. J., "Numerical simulation of the interaction between turbulence and radiation in reactive flows", *Prog. Energy Comb. Sci.*, **33**, 311, (2007).

[15] Warnatz, J., Maas, U., Dibble, R.W., Combustion-Physical and chemical fundamentals, modeling and simulation, experiments, pollutant formation, 4th ed., Springer, (2006).

[16] Yakhot, V., Orszag, S. A., Thangam, S., Gatski, T. B., Speziale, C. G., "Development of turbulence models for shear flows by a double expansion technique". Physics of Fluids A, 4, 1510, (1992).

[17] Choudhury, D. Introduction to the Renormalization Group Method and Turbulence Modeling. Fluent Inc. Technical Memorandum TM-107, (1993).

[18] Versteeg, H. K. Malalasekera, W. An introduction to computational fluid dynamics: the finite volume method. Addison Wesley-Longman, (1995).

[19] Westbrook C. K., Dryer, F. L., "Simplified reaction mechanisms for the oxidation of hydrocarbon fuels in flames". Combust. Sci. Tech., 27, 31, (1981).

[20] Mallard, W. G., Westley, F., Herron, J. T., & Hampson, R. F. NIST chemical kinetics database. Gaithersburg, MD, USA: National Institute of Standards and Technology Standard Reference Data. http://www.nist.gov/srd/, (2003).

[21] Kang, J., Cheng, P., "Two-dimensional radiating gas flow by a moment method". AIAA J., 2, 1662, (1964).

[22] Christo, F. C., Dally, B. B., "Modeling turbulent reacting jets issuing into a hot and diluted coflow", Combust. Flame, 142, 117, (2005).

[23] Coppens, F. H. V., De Ruyck, J., Konnov, A. A., "Effects of hydrogen enrichment on adiabatic burning velocity and NO formation in methane + air flames", *Exp. Thermal Fluid Sci.*, **31**, 437, (2007).